IDENTIFYING ABBERANT SEGMENTS IN PERMANENT DOWNHOLE GAUGE DATA

A REPORT SUBMITTED TO THE DEPARTMENT OF ENERGY RESOURCES ENGINEERING OF STANFORD UNIVERSITY

IN PARTIAL FULFILLMENT OF THE REQUIREMENTS FOR THE DEGREE OF MASTER OF SCIENCE

By
Emuejevoke Origbo
June 2010

I certify that I have read this report and that in my opinion it is fully adequate, in scope and in quality, as partial fulfillment of the degree of Master of Science in Petroleum Engineering.

_____

Prof. Roland Horne
(Principal Advisor)

Abstract

Data from permanent downhole gauges are needed for interpretation of subsurface conditions in a well. The data from permanent downhole gauges are voluminous and usually contains aberrant segments. Using this aberrant data to characterize the reservoir leads to generation of inaccurate reservoir parameters (permeability, skin and storage).

The approach used in this work to solve the problem of interpretation of permanent downhole gauge data was by generation of multisegment synthetic pressure data using the pressure equation with all the reservoir parameters known. An aberration was introduced in the form of a pressure segment that went against the reservoir physics; it decreased with a production shut in, when it should increase. An algorithm based on direct Kalman filtering technique was developed which was independent of the reservoir model and extracted a signal with the minimum error (mean square deviation) from the noisy/aberrant signals. In this way, aberrant segments were successfully identified, removed and the original signal with actual reservoir parameters recovered.

Acknowledgments

I am grateful to the member companies of SUPRI-D for financial support for this work.

To my advisor, Professor Roland Horne for his advice, patience and mentorship throughout the course of my work, I say thank you.

To Professor Hamdi Tchelepi, thank you for your encouragement.

To my friends at the department of Energy Resources Engineering, thank you for making my work enjoyable.

To my parents, I say thank you for your support throughout the years. Darlington, Ufuoma, Efesa and Jite, you are the best siblings in the world!

Daniel Elstein, the single best thing to happen to me; thank you for making me laugh and for causing time to pass effortlessly. I am because we are…

Contents

List of Figures

Chapter 1

Introduction

1.1. Background

In 1972, Schlumberger installed the first permanent downhole gauge on logging cable in West Africa. Today, there are over 7000 permanent downhole gauge installed in wells all over the world supplying continuous real time data about subsurface reservoir conditions. Permanent downhole gauges are used in reservoir monitoring and management by interpreting the pressure, flow rate and temperature data read from the gauges.

Data from the gauges are voluminous and since they are collected over long periods of time, prone to errors. Making decisions based on the data without first removing these errors may lead to wrong conclusions being reached on the reservoir conditions. There is a need to validate the gauge data by comparing with expected pressure transients generated using the flow rate data. After the comparison, the data can be improved by removing segments of the data that are aberrant.

1.2. Problem Statement

Several attempts have been made to interpret data from permanent downhole gauges. These attempts have utilized pressure data from permanent downhole gauges directly without performing the critical first step of aberrant segments removal. Flow rate and pressure data were analyzed together in these studies.

Table 1-1: Reservoir parameters matched using aberrant and filtered data. Reproduced from Athichanagorn (1999)

Parameter	Actual values	First match	Final match
Permeability, k	100	126.38	98.93
Skin, S	3	5.14	2.91
Storage, C	0.05	0.0555	0.0502
Reservoir radius, re1	500	384.55	531.97
Reservoir radius, re2	1000	1028.67	975.08

As shown in Table 1-1, an illustration from Athichanagorn (1999), interpretation of pressure data with aberrant segments led to inaccurate estimates of reservoir parameters. The original parameters from which Figure 1-1 was generated are shown in the second column of Table 1-1. The first match achieved, without filtering the signal was calculated as shown in the third column of Table 1-1. There was a marked distinction between the first match and the actual reservoir values. As the signal was successively filtered a close match was made between the filtered data and the original reservoir parameters. The final match of the reservoir parameters were reasonably approximations to the actual values.

The original data with aberrant segments and the fitted data with close estimates of actual reservoir parameters were plotted as shown in Figure 1-1. The fitted data signal was generated using the values derived from the final match. The method used in filtering the data will not be discussed here. Although this was a multisegment signal with only two aberrant segments, the effect on reservoir parameter estimation was significant. In the case of field data from permanent downhole gauges with many hours of production and several pressure transients, the error in the parameters estimated would be magnified. In

this study, the pressure transient data was filtered to identify aberrant segments. Initially, the method chosen to identify aberrant segments was the visual characteristics method combined with the *ratio of derivatives* method. However, due to limitations of these methods, several other methods were tested. As will be shown in subsequent chapters, the Kalman filter technique was found to identify aberrant segments satisfactorily in multisegment pressure data.

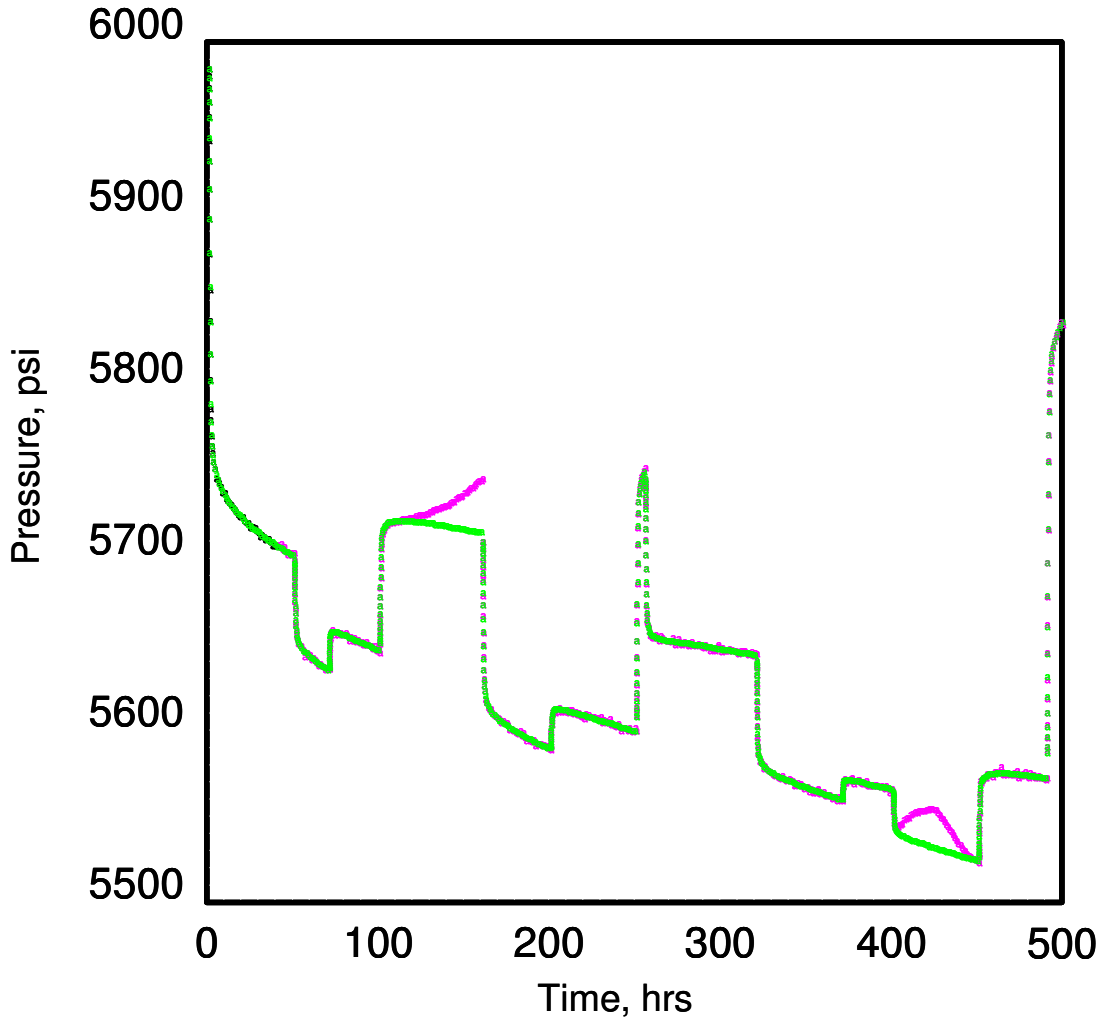

Figure 1-1: Pressure Data showing original and fitted data. Reproduced from Athichanagorn (2000)

Chapter 2

Literature Review

Over the last decade, several authors have developed methods of interpreting data from permanent downhole gauges. These methods have improved the use of gauge data in reservoir management significantly. Gilly and Horne (1998) studied the integration of flow rate history and pressure history data in well test analysis. The study used the convolution equation, Laplace transforms and deconvolution to increase the quality and quantity of information extracted from pressure data. In addition, the study provided a means for interpretation of a longer pressure response.

Athichanagorn (1999) developed a seven step approach. Athichanagorn (1999) utilized the convolution equation, wavelets, Fourier transform, regression analysis and data selected with a sliding window in interpreting data from permanent downhole gauges. Athichanagorn (1999) detected outliers in the data, denoised the data and identified both abberant transients and break points.

Thomas (2002) conducted work in aberrant transient removal from permanent downhole gauge data. Thomas (2002) utilized the convolution equation, regression analysis and the pressure equation. A pattern-recognition technique was developed which aided removal of aberrant transients. Furthermore, Thomas (2002) proposed that the pressure derivative data be analyzed on a logarithmic scale to aid in removal of aberrant transients in gauge

data. In this current study, the method proposed by Thomas (2002) was explored as the *ratio of derivatives* method.

Nomura and Horne (2009) utilized wavelets, deconvolution and visual characteristics in transient identification and flow rate estimation. A method of identifying break points in transient data was developed.

Welch and Bishop (2006) provided an introduction to a technique used in interpreting pressure signals, the Kalman filter: "The Kalman filter is a set of mathematical equations that provides an efficient computational (recursive) means to estimate the state of a process, in a way that minimizes the mean of the squared error". The Kalman filter has been applied in signal processing in the fields of medicine and engineering.

In the medical field the Kalman filter has been used to interpret blood flow rate from heart monitoring devices and pressure in arteries of the heart. In the field of engineering, the Kalman filter has been used in aerospace engineering for tracking the trajectory of satellites. The Kalman filter has also been utilized in the earth sciences in interpretation of seismic and pressure data and in predicting pressure data profiles from reservoirs.

Yu et al. (2009), studied leakage detection in crude oil pipelines. Yu et al. (2009) interpreted pressure and flow rate signals using the combined Kalman filter-discrete wavelet transform method. The result of the study was a method for denoising pressure data and for extracting leakage locations in crude oil pipelines based on the extracted filtered signal.

Chapter 3

Methodology

3.1. Data Generation

A relationship exists between the flow rate history and the pressure history that is based on the reservoir physics. That relationship was used in this work in generating synthetic pressure data with known reservoir parameters using the pressure equation given as Equation (3.1).

$$p_{wf} = p_i - \left(\frac{162.6qB\mu}{kh}\right)\times\left(\log(t)+\log(\frac{k}{\phi\mu c_t r_w{}^2})+0.8686s-3.2274\right) \quad (3.1)$$

Three assumptions were made regarding the reservoir conditions in this study:

- Flow rate data is noiseless and constant in each time step;
- Flow rate represents the reservoir physics accurately;
- Break points are known for each pressure transient.

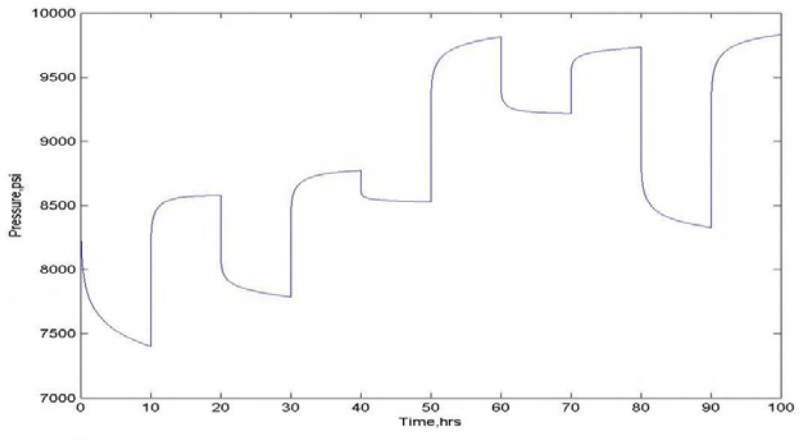

Figure 3-2: Synthetic pressure data

Typically, a draw-down response is recorded from a reservoir during production. As production is decreased or stopped, a pressure build-up response is recorded as shown in Figure 3-2.

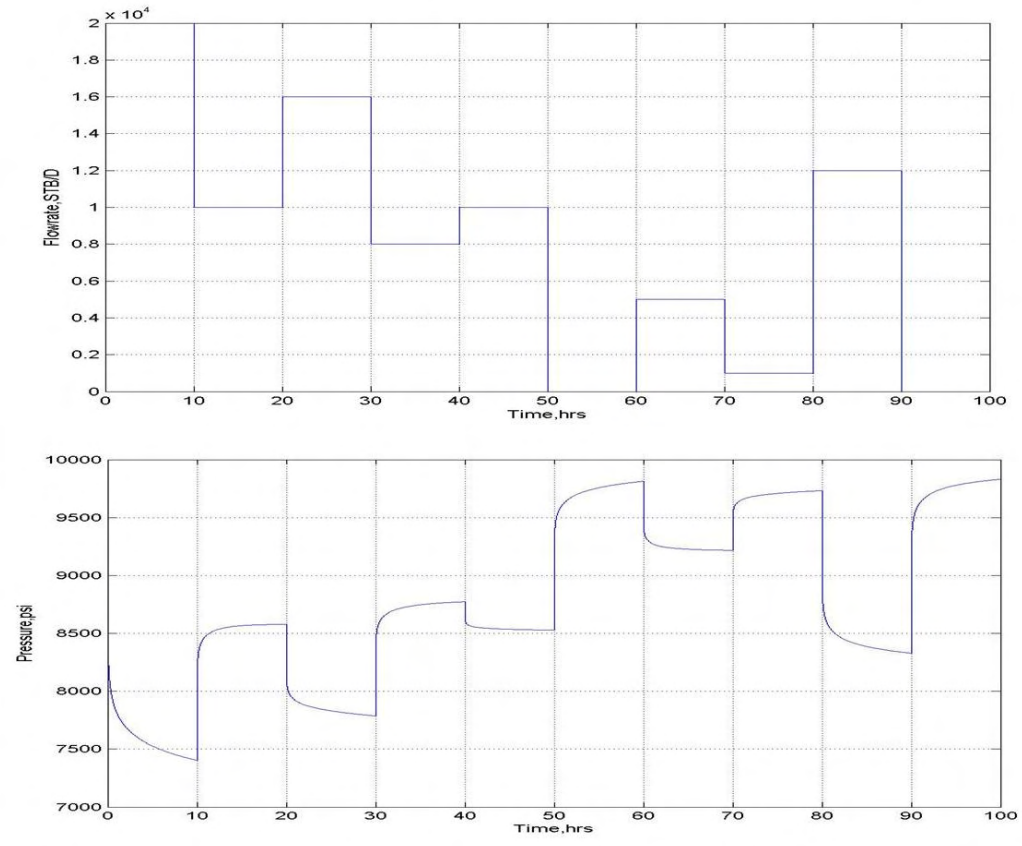

Figure 3-2: Synthetic flow rate data with corresponding pressure data.

To investigate the presence of aberrant segments in the pressure data, an aberration was introduced and superimposed in the fifth time step (40 hour-50 hour) as shown in Figure 3-3. A method was developed to identify this aberration. The method utilized in identifying aberrations in the pressure data was the application of a pattern recognition technique based on visual characteristics as stated in previous literature.

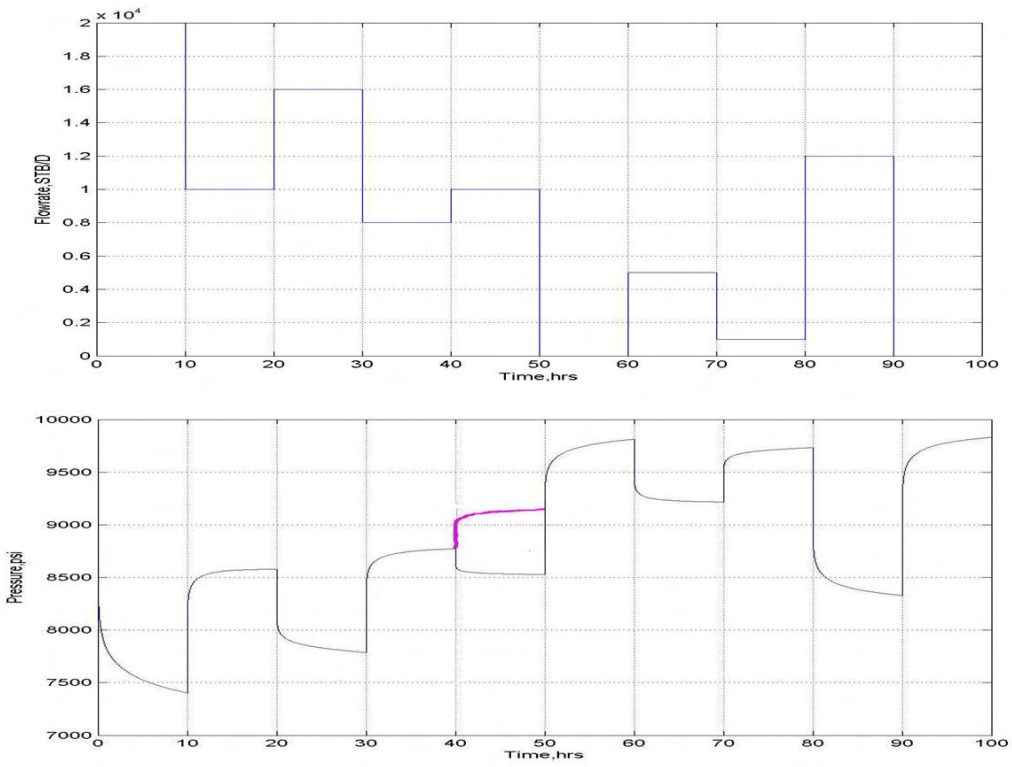

Figure 3-3: Synthetic flow rate data with corresponding pressure data superimposed with an aberrant segment.

Visually, it was possible to identify the aberrant segment. A further investigation explored was the possibility of aberrations in segments of the pressure data that appeared to obey the reservoir physics. The curves for draw down and build up of the pressure data were all tested to ascertain if the steepness of the curves matched expected reservoir responses at corresponding time steps. The test was to determine the degree of compliance of these segments with the reservoir physics.

3.2. Degree of Aberration

To calculate the degree of aberration in the pressure transients, the pressure derivatives and the flow rate derivatives were computed for each time step. The *ratio of derivatives*

method was then introduced. As the name suggests, the method involves computing the ratio of the pressure derivative and that of the flow rate derivative with the pressure derivate taken as the denominator. From Figure 3-3, as flow rate increased pressure decreased. Thus, a negative pressure derivative was calculated for the case of increasing flow rate. The flow rate derivative, as flow rate increased was positive. On the other hand, a flow rate decrease or stoppage resulted in an increase in pressure. A positive pressure derivative was calculated for the case of decreasing flow rate. The flow rate derivative, as flow rate decreased was negative.

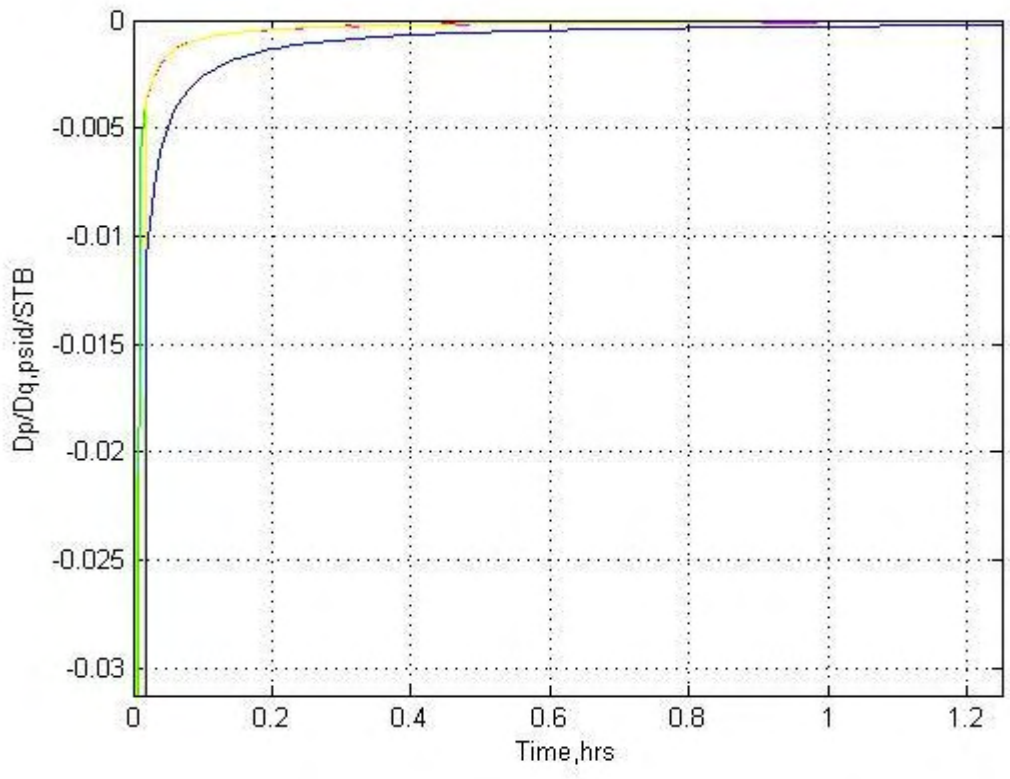

Figure 3-4: Ratio of pressure and flow rate derivative versus time super-imposed on one another.

Applying the *ratio of derivatives* method, a negative number was calculated each time as the pressure and flow rate derivatives for each time step had alternate signs. A plot of the ratio of derivates versus time step is given in Figure 3-4. The time steps were of equal

lengths of ten hours and the plots for each time step was super-imposed on the plot for the previous time step to allow for visual comparison. As time increased past one hour, no significant visual characteristic differences were observed in the combined plot of each time step. A closer look was taken of the section on the ratio of derivatives curve where the curves did not fully overlap. The differences in the plots of the various time steps were quite subtle.

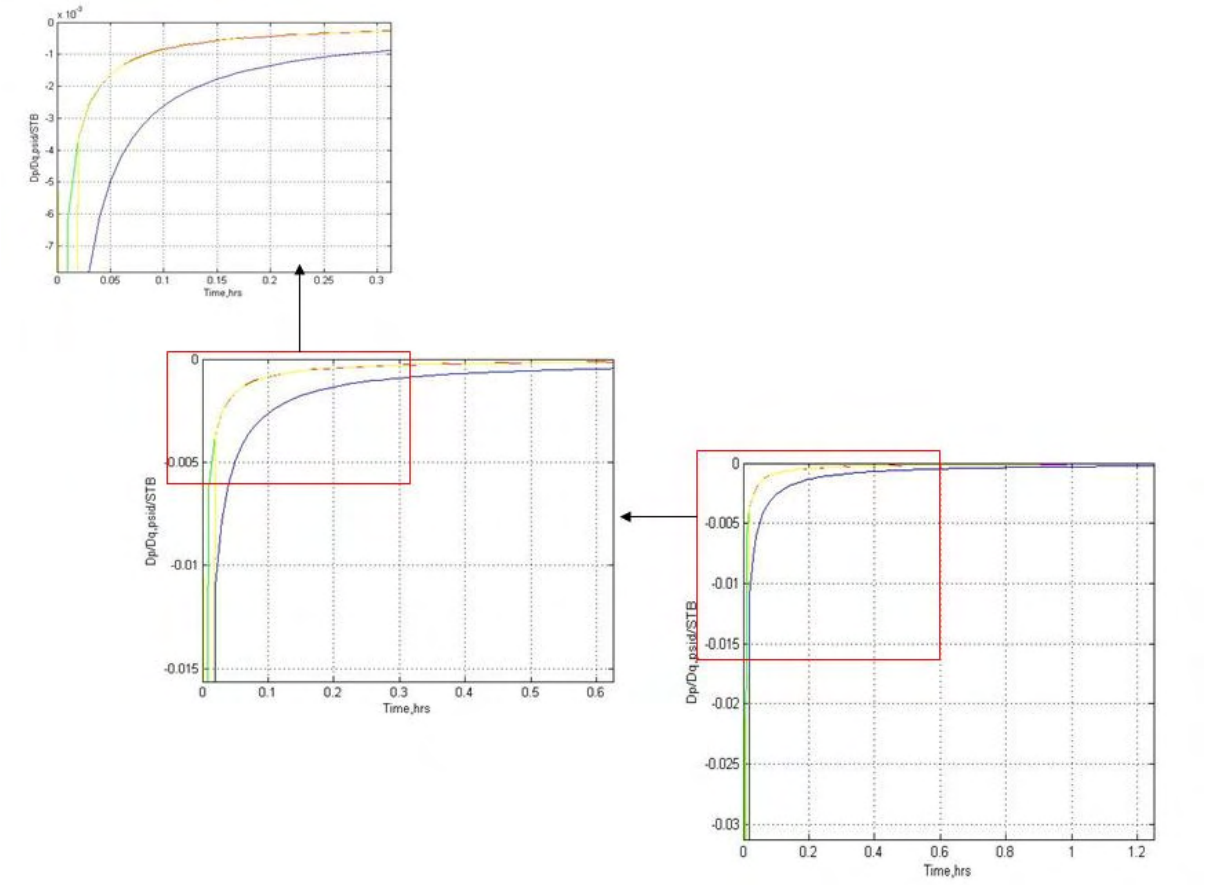

Figure 3-5: Close-up of ratio of pressure and flow rate derivative versus time super-imposed on one another.

As expected, in the segment of the pressure data where the aberration was introduced as in Figure 3-3, the ratio of the derivatives was positive. In this segment, increased flow

rate response corresponded to an increased pressure response. Thus the ratio of the derivatives for this time step was positive as shown in Figure 3-6.

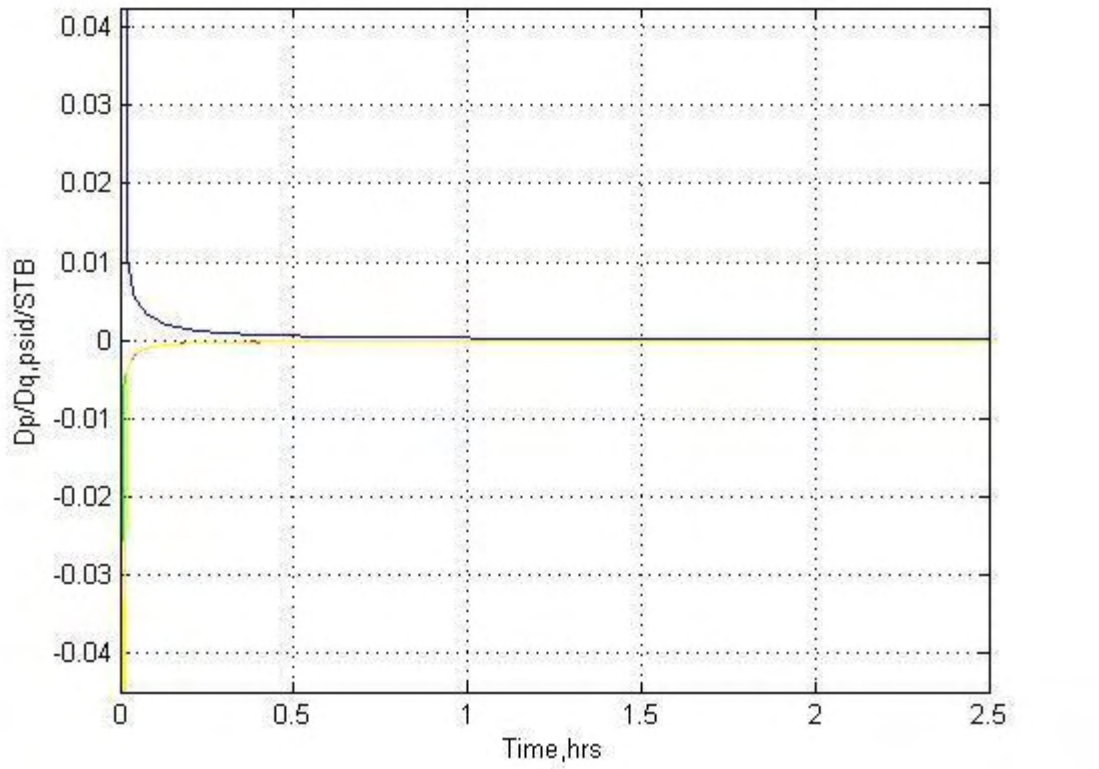

Figure 3-6: Ratio of pressure and flow rate derivative versus time (including the aberrant segment time step), superimposed on one another.

After utilizing the visual characteristic method, to better estimate the degree of aberration in each pressure transient, the mean squared deviation between transients was calculated. The results were stored as elements of a matrix. The matrix generated was a symmetric matrix with zero on the diagonal as each element is exactly similar to itself. However, it was difficult to set a threshold mean squared deviation value from which to establish the degree of aberration, as the values were small and setting the threshold would be a highly subjective process.

To overcome this challenge, a new method was sort to identify aberrations in pressure transients. Studies suggested that the Kalman filter was "an efficient computational (recursive) means to estimate the state of a process, in a way that minimizes the mean of the squared error", Welch and Bishop (2006). As it was necessary to compute the mean of the squared error in this work without recourse to a subject method of determining aberration in pressure data, the Kalman filter was used to identify aberrant segments.

3.3. The Kalman Filter

The Kalman filter estimates the state x of a discrete-time controlled process that is governed by a linear stochastic difference equation. The Kalman filter consists of two main components:

- A discrete process model, described by a linear stochastic difference equation which relates a change in state with time;

$$x_k = Ax_{k-1} + w_k \tag{3.2}$$

- A measurement model described by a linear function which establishes the relationship between the state of a process and a measurement.

$$z_k = Hx_k + v_k \tag{3.3}$$

$\boldsymbol{A}$ is the matrix ($n \times n$), that describes how the state evolves from time k to $k-1$ without noise.

$\boldsymbol{H}$ is the matrix ($m \times n$) that describes how to map the state x_k to an observation z_k

w_k and v_k are random variables representing the process and measurement noise that are assumed to be independent and normally distributed with covariance R_k and Q_k respectively.

$\hat{\mathbf{x}}_k \in \Re^n$ is the estimated state at time step k and $\hat{\mathbf{x}}_k^- \in \Re^n$ is the state after prediction before observation.

$$\mathbf{e}_k^- = \mathbf{x}_k - \hat{\mathbf{x}}_k^- \tag{3.4}$$

$$\mathbf{e}_k = \mathbf{x}_k - \hat{\mathbf{x}}_k \tag{3.5}$$

The calculated errors are given by Equations (3.4) and (3.5). The error covariance matrices are calculated using Equations (3.6) and (3.7).

$$\mathbf{P}_k^- = E[\mathbf{e}_k^- \mathbf{e}_k^{-T}] \tag{3.6}$$

$$\mathbf{P}_k = E[\mathbf{e}_k \mathbf{e}_k^T] \tag{3.7}$$

The Kalman filter estimates $\hat{\mathbf{x}}_k$ and $\mathbf{P}_k$.

In this study, the pressure transient data from the permanent downhole gauges were assumed stationary. The form of the time update equation also known as the predictor equations, used is given by Equation (3.8). This form of the equation does not update the state with time and the matrix $\mathbf{A}$ is the identity matrix. The update error covariance matrix $\mathbf{P}$ is given by Equation (3.9).

$$\hat{\mathbf{x}}_k^- = \mathbf{A}\hat{\mathbf{x}}_{k-1} \tag{3.8}$$

$$\mathbf{P}_k^- = \mathbf{A}\mathbf{P}_{k-1}\mathbf{A}^T + \mathbf{Q} \tag{3.9}$$

The measurement equation, also called the corrector equation used to calculate the expected value of $\mathbf{x}$ is given by Equation (3.10). The update error covariance matrix is calculated using Equation (3.11).

$$\hat{\mathbf{x}}_k = \hat{\mathbf{x}}_k^- + \mathbf{K}_k(\mathbf{z}_k - \mathbf{H}\hat{\mathbf{x}}_k^-) \tag{3.10}$$

$$\mathbf{P}_k = (\mathbf{I} - \mathbf{K}_k \mathbf{H})\mathbf{P}_k^- \tag{3.11}$$

The optimal Kalman gain $\mathbf{K}_k$ was calculated using Equation (3.12).

$$\mathbf{K}_k = \mathbf{P}_k^- \mathbf{H}^T (\mathbf{H}\mathbf{P}_k^- \mathbf{H}^T + \mathbf{R})^{-1} \tag{3.12}$$

The Kalman filter operates as a series of predictions, using the time update, and corrections, using the measurement update, to estimate the expected value of the state of a system.

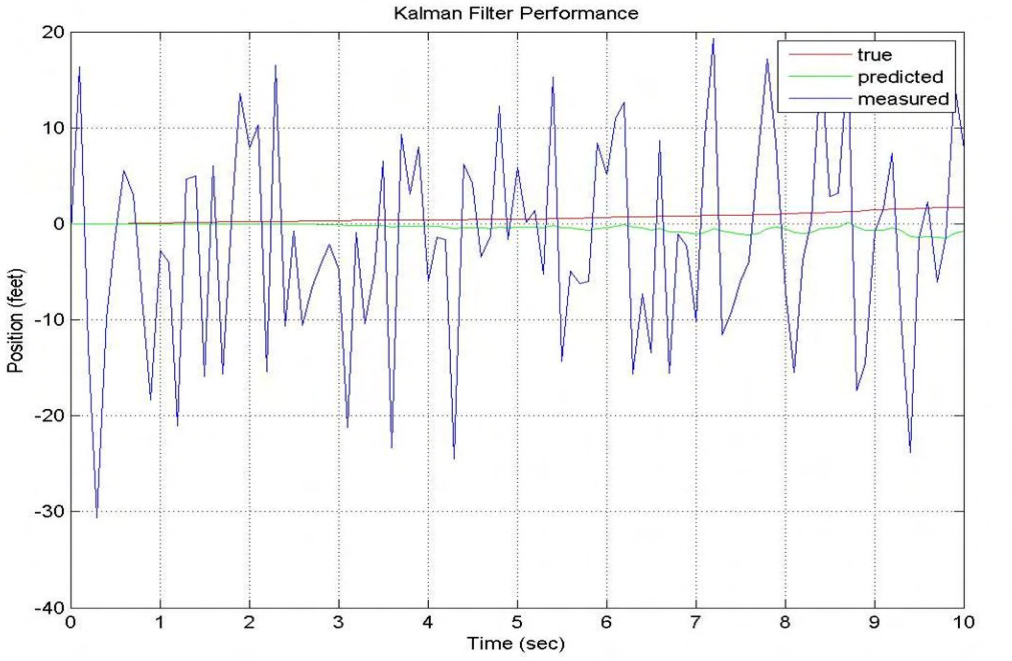

Figure 3-7: Position of a car estimated using the Kalman filter. Reproduced from Simon (2009).

In the example illustration in Figure 3-7, a series of noisy measurements of the position of a car were filtered using the Kalman filter. The filtered signal, the actual signal and the measured signal are referred to as predicted, true and measured respectively. This example is analogous to the problem being solved in this work. The pressure data from the permanent downhole gauge is similar to the noisy measurements of the position of a car, the measured data. The true data could be taken as the synthetic pressure data

generated and the predicted position of the car, the filtered pressure signal. The problem of identifying aberrant segments in permanent downhole gauge data was solved with a method analogous to that used to generate the illustration in Figure 3.7.

In this study, x_k and z_k are the actual pressure transient data and measured pressure transient data respectively. **H** is the flow rate data. Q the process noise covariance and R, the measurement noise covariance control the effectiveness of the filter. The ratio Q/R should be relatively small to ensure optimal reproduction of the actual data by the Kalman filter. The predicted data is generated by substituting the pressure kernel x_k and the flow rate data, **H** in Equation (3.3).

In implementing the Kalman filter algorithm, the flow rate was assumed constant for each time step. Each column in the matrix of flow rate data, **H**, was generated as a vector of constants for each time step. The pressure kernel is extracted from the pressure transients by utilizing the Matlab Kalman toolbox as developed by Murphy (1998). To generate the pressure kernel, Equation (3.1) takes the form given below:

$$y_t = Iy_{t-1} + w_t \qquad \text{for } t = 1\ldots\ldots n \tag{3.13}$$

The pressure kernel, x_k and the flow rate are substituted in Equation (3.3) to solve for the predicted data from the noisy measurements and Equation (3.3) takes the form of Equation (3.14). The matrix **H** is as given in Equation (3.15).

$$p_t = Hy_t + v_t \qquad \text{for } t = 1\ldots\ldots n \tag{3.14}$$

$$H = \begin{bmatrix} q_1 & \cdots & q_n \\ \vdots & \vdots & \vdots \\ q_1 & \cdots & q_n \end{bmatrix} \tag{3.15}$$

Chapter 4

Results

The Kalman filter was used to denoise synthetic data generated using known reservoir parameters and to identify sections of the data with aberrant segments. Three cases were examined in this study.

- Case1: Filtering pressure data with 5% Gaussian noise using the Kalman filter;
- Case 2: Identifying an aberrant segment introduced in the pressure data in Case 1;
- Case 3: Sensitivity analysis of Case 1 with 5% Gaussian noise introduced in the flow rate data.

For Case 1, synthetic pressure data representing the pressure data from a permanent downhole gauge was generated and labeled true data. 5% Gaussian noise was added to the generated synthetic pressure data and labeled measured data. The Kalman filter was then used to filter the measured data and the result labeled filtered data. These results are shown in Figure 4-1. In addition, plots of the pressure kernel corresponding to the true, measured and filtered data were generated. These plots of the pressure kernels are the key makers for determining if an aberrant segment was present in the data or not. The aberrant segments were identified using a pattern recognition method.

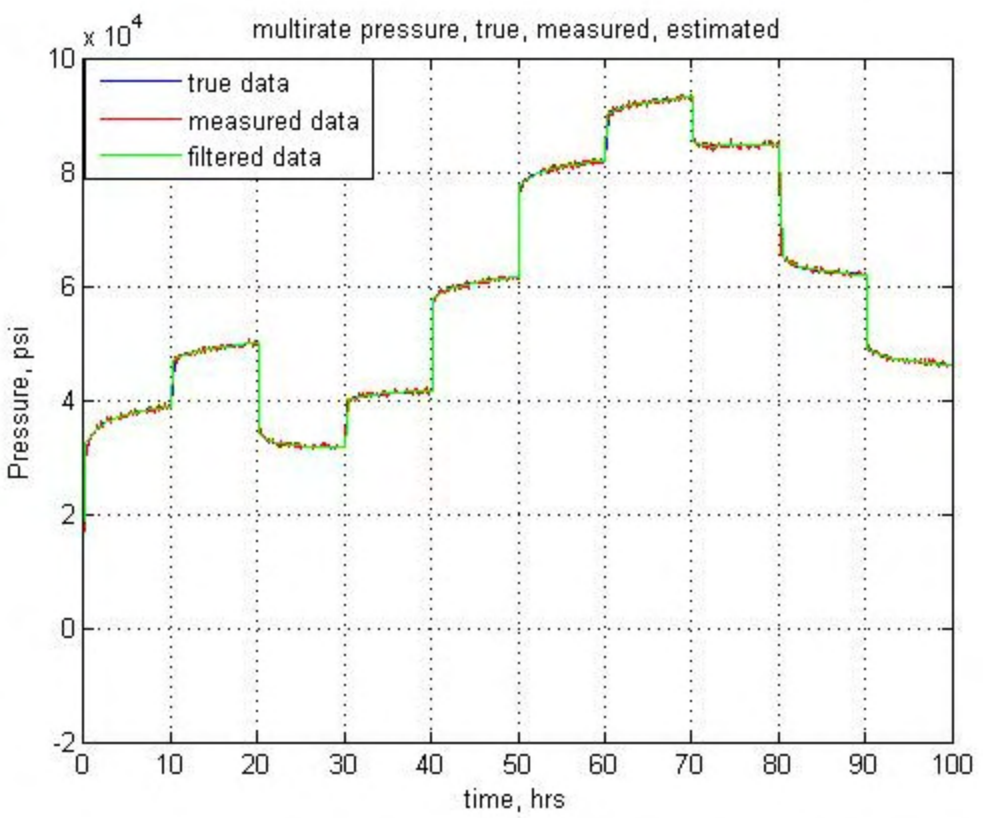

Figure 4-1: True, measured (noisy) and filtered (denoised) pressure data.

The pressure kernel plots for the true and measured data were plotted together to aid visual comparison as shown in Figure 4-2. Any visual discrepancies in the plot of the pressure kernel generated from pressure data with that of the expected kernel plot as shown in Figure 4-3, was taken to signify the possibility of an aberration in the pressure data.

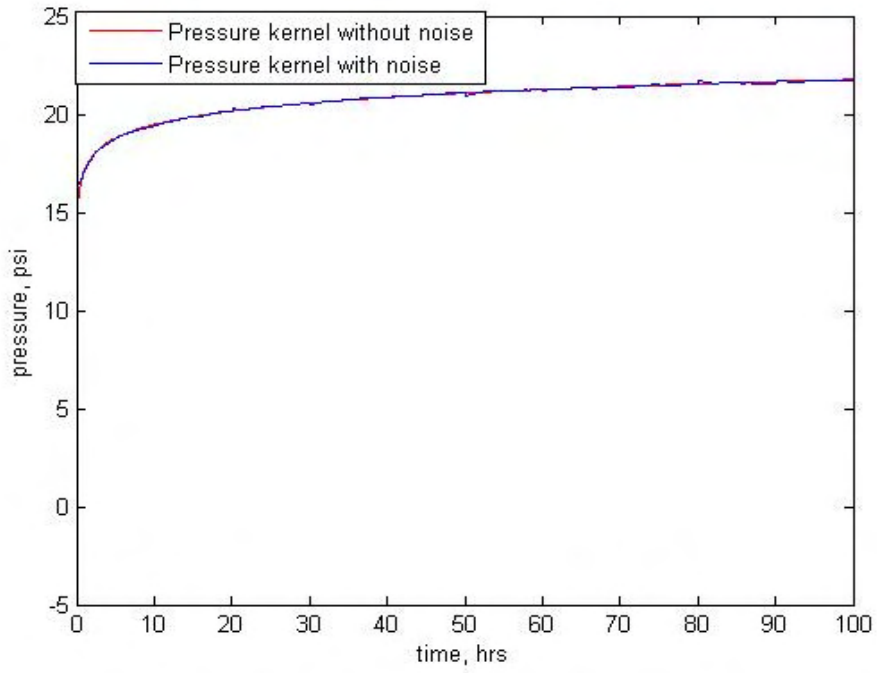

Figure 4-2: Pressure kernel for true (synthetic) and measured (noisy) data.

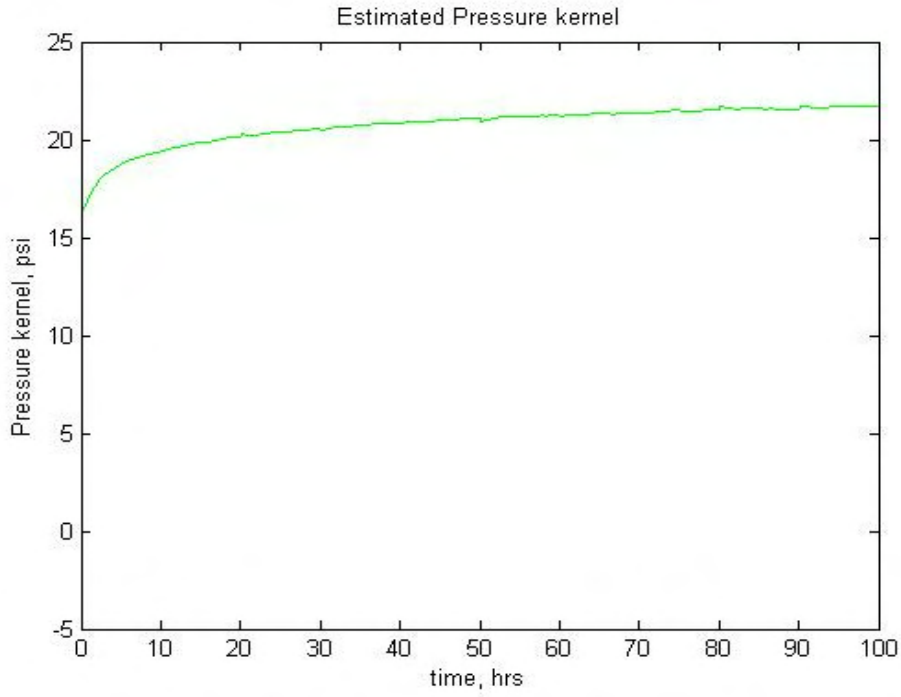

Figure 4-3: Estimated pressure kernel using the Kalman filter.

In Case 2, an aberration was added in the 60-70 hour segment of the measured pressure data used in Case 1 in the form of a pressure segment that went against the reservoir physics as shown in Figure 4-4. The Kalman filter was applied and the plots of the pressure data, true, measured and filtered, given as shown in Figure 4-4.

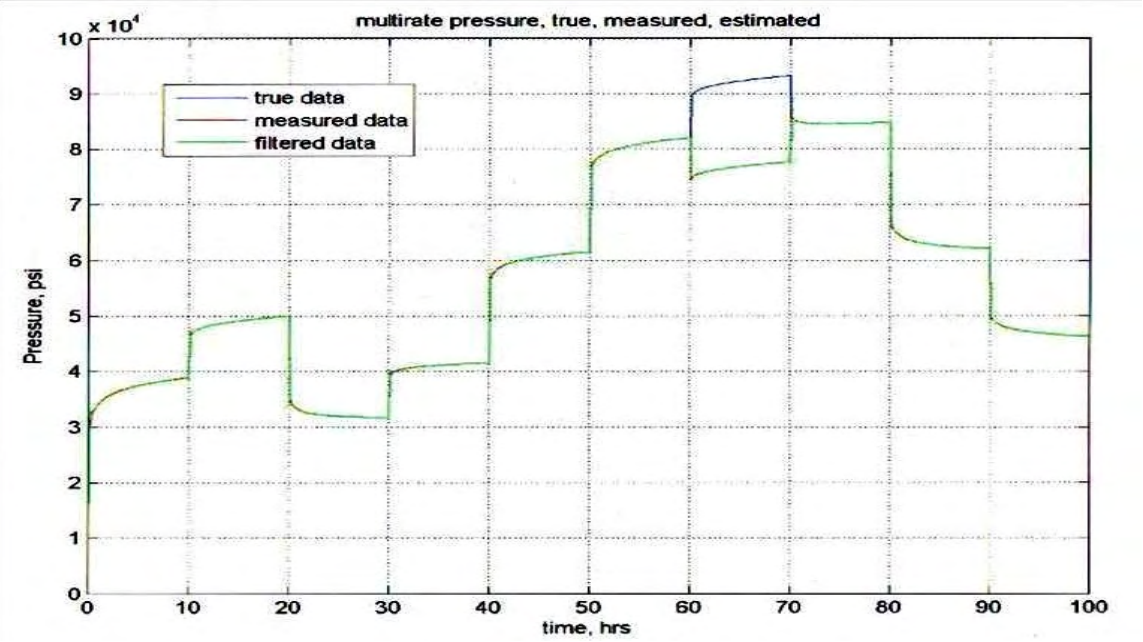

Figure 4-4: True, measured (noisy) and filtered (denoised) pressure data with aberration starting at the 6th time step (60-70hours).

The Kalman filter accurately filtered the measured data and reproduced a pressure signal profile that matched the measured data. The pressure kernel plots for the true and measured data shown in Figure 4-5 displayed instability in the pressure kernel plots beginning at 60 hours that continued till the end of the signal run at 100 hours. The approach used to search for the aberration in the pressure data was to clip out the time step at which the aberration was first noticed and to remove time steps sequentially after

that until the aberration was identified. The evidence of successful identification of the aberrant segment was a return to stability of the pressure kernel plot.

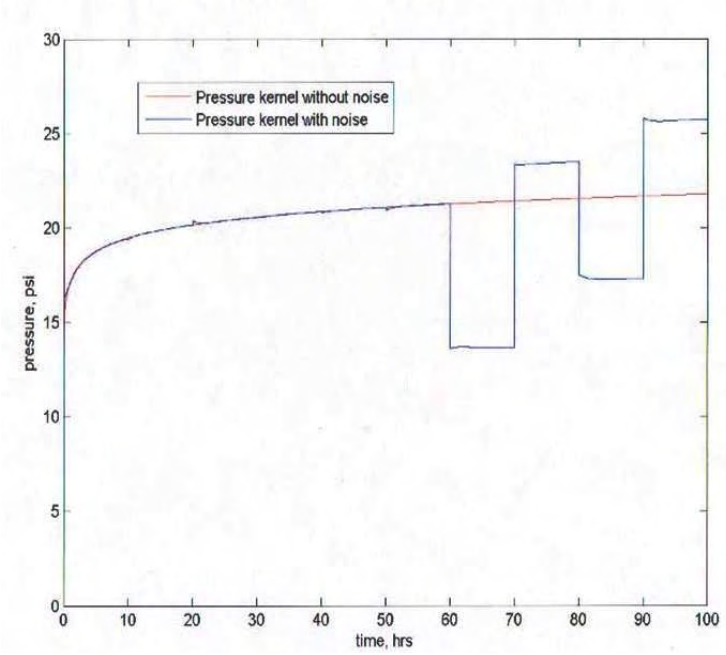

Figure 4-5: Pressure kernel for true (synthetic) and measured (noisy and aberrant) data.

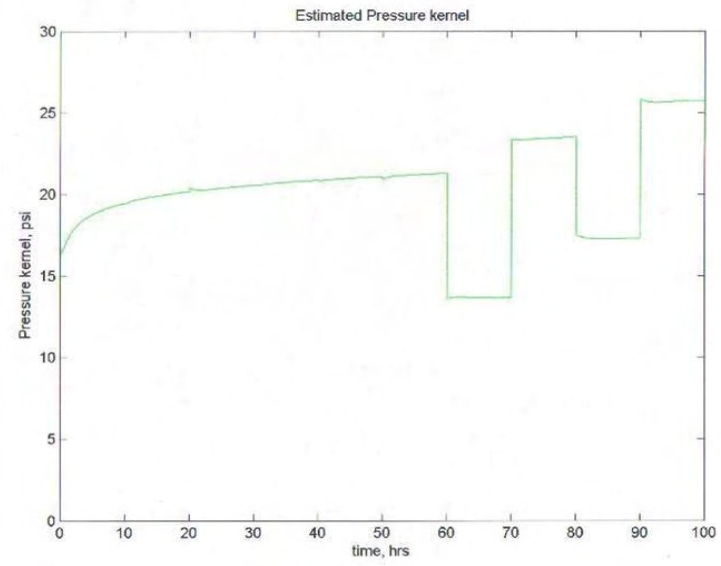

Figure 4-6: Estimated pressure kernel using the Kalman filter.

The removal of the pressure data segment in the time step in which the aberration was first noticed caused the pressure kernel curve to immediately stabilize as shown in Figures 4-7 and 4-8 respectively.

A check was made by moving the aberration to different time steps and observing the effect on the pressure kernel plot. In each of the cases with the aberration in different time steps, a similar response to that observed in Case 2 was recorded. Instability in the pressure kernel plot was noticed which signified the presence of an aberrant segment in the pressure data. Clipping out the time step at which the aberration was first noticed led to removal of the aberrant segment.

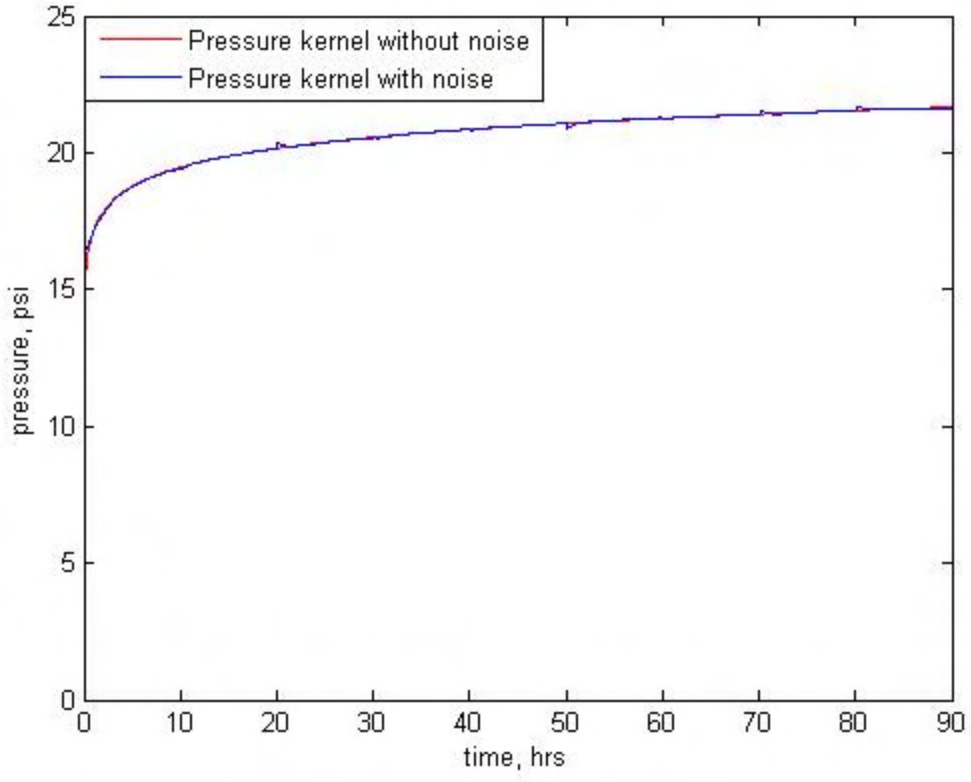

Figure 4-7: Pressure kernel for true (synthetic) and measured (clipped) data.

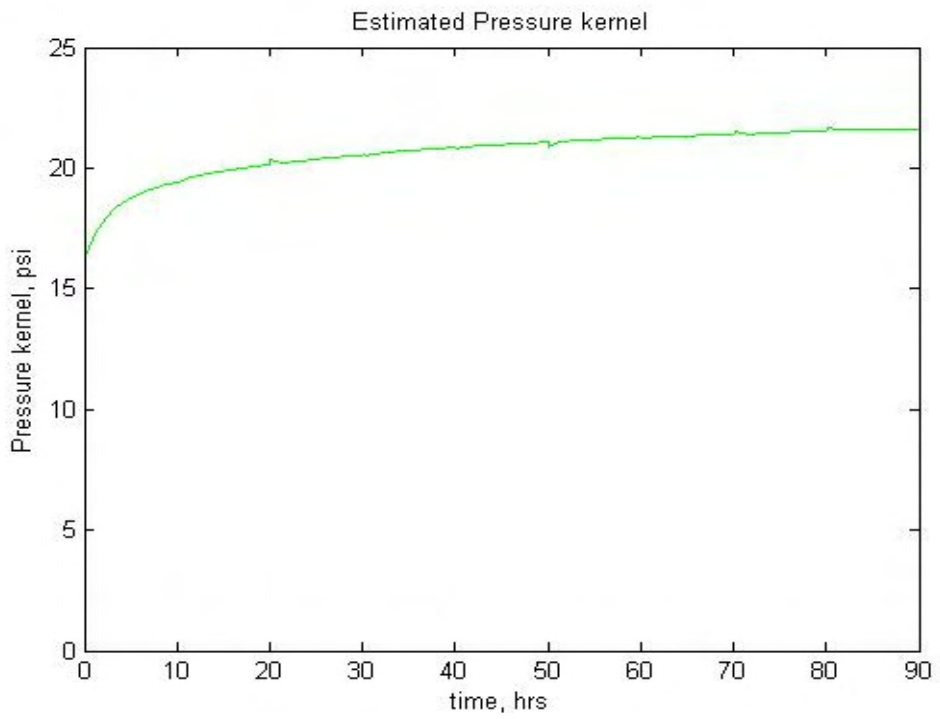

Figure 4-8: Estimated pressure kernel using the Kalman filter.

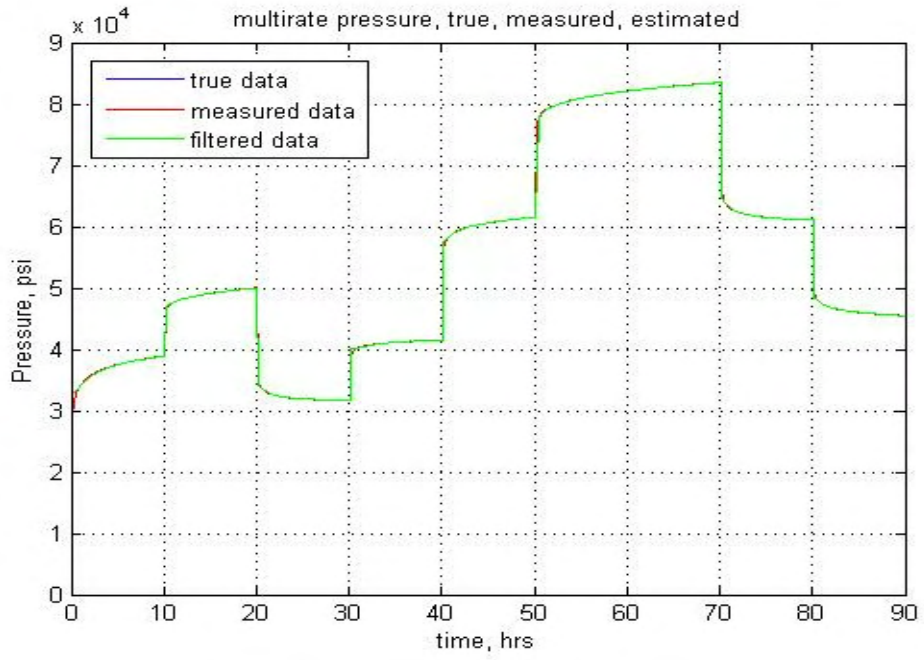

Figure 4-9: Estimated pressure kernel using the Kalman filter.

The full plot of the pressure transient data after removing the aberrant segment from Figure 4-4 is given in Figure 4-9.

Case 3, a sensitivity analysis on the synthetic pressure data, was carried out to investigate the effect of the presence of noise in the flow rate data used to generate the pressure data in case 1. 5% Gaussian noise was introduced in the flow rate data. The presence of noise in the flow rate data did not change the response of the pressure data to the filter algorithm as shown in Figures 4-10, 4-11 and 4-12 respectively. The only observable difference between Figures 4-1, 4-2 and 4-3 and Figures 4-10, 4-11 and 4-12 respectively, is the presence of the rises and falls in the pressure data plot. No difference was observed in the plot of the pressure kernel curves for Case 3 from that of Case 1.

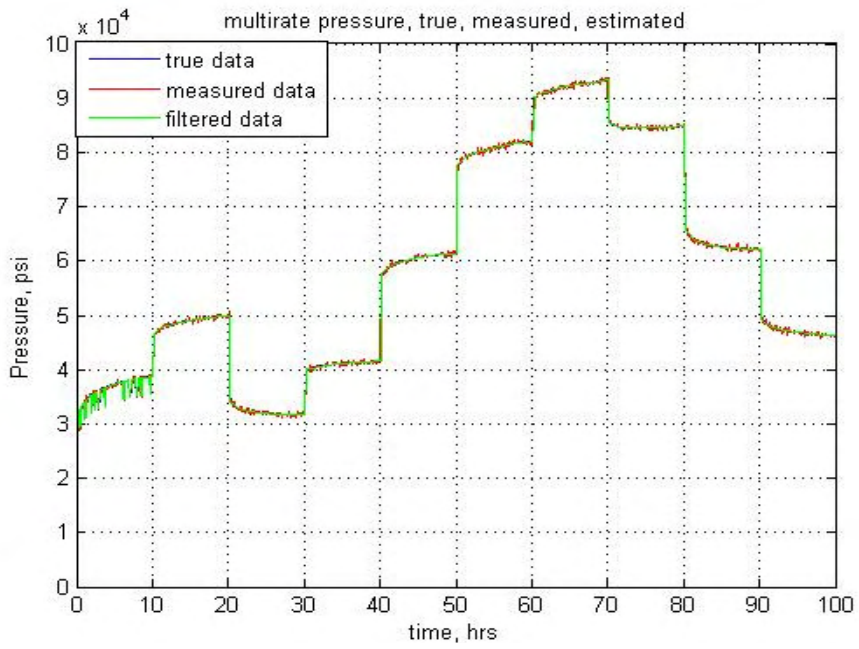

Figure 4-10: True, measured (noisy) and estimated pressure data.

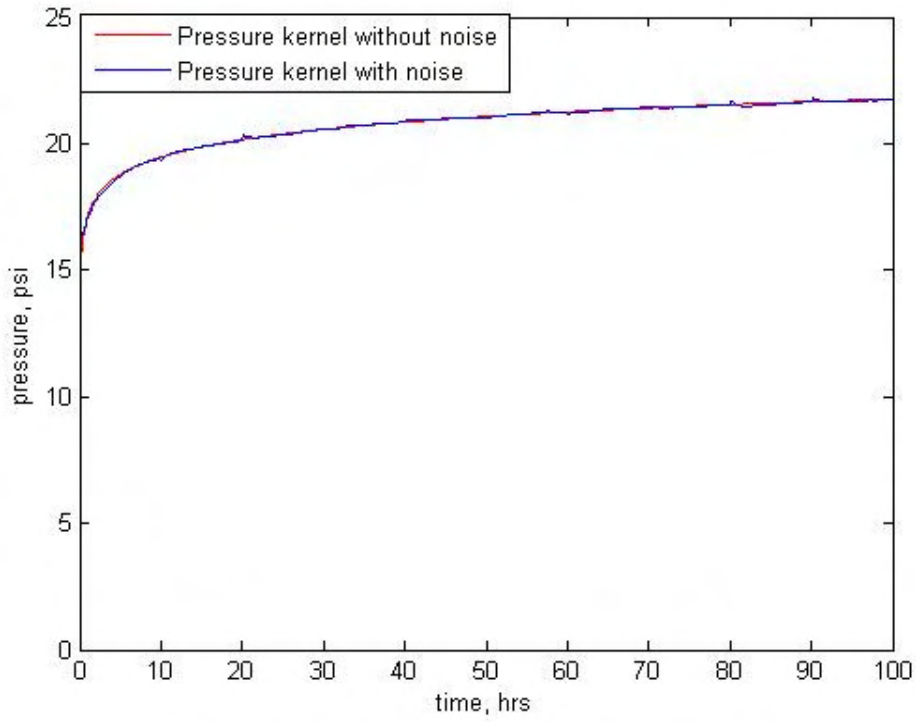

Figure 4-11: Pressure kernel for true (synthetic) and measured (noisy) data for Case 3.

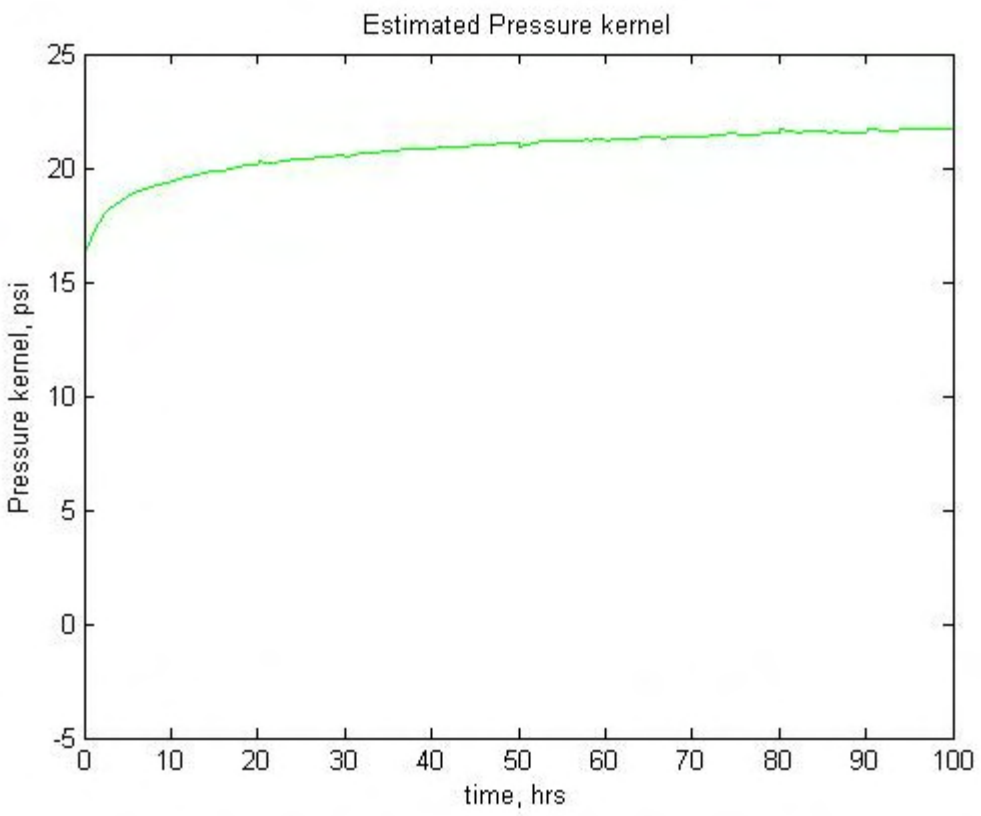

Figure 4-12: Estimated pressure kernel for Case 3 using the Kalman filter.

Chapter 5

Conclusion and Recommendation

5.1 Conclusion

Aberrant segments in permanent downhole gauge data were identified and removed. The results from this study serve as a necessary first step in any interpretation of pressure and flow rate data from permanent downhole gauges. The Kalman filter and the method of deconvolution were utilized in identifying the aberrant segments.

5.2 Recommendation for Future Work

In this study, the flow rate data were assumed accurate in all cases. The flow rate data were then used to predict what the pressure data should be. When the pressure data did not match the flow rate data prediction pressure profile, it was assumed to be aberrant. However, in the field, flow rate data would often be inaccurate. The reverse case should be simulated; the case of pressure being assumed accurate and sections of the flow rate data that go against the reservoir physics, termed aberrant.

In addition, in this study, the reservoir parameters were assumed constant with time; stationary. The scenario of reservoir parameters changing with time should be simulated.

Nomenclature

A = state transition matrix

B = formation volume factor (res vol/std vol)

c_t = total system compressibility (/psi)

e_k = error vector

h = thickness (ft)

H = measurement matrix

k = time

K = Kalman gain matrix

p_i = initial reservoir pressure (psi)

P = update error covariance matrix

p_{wf} = well flowing pressure (psi)

q = flowrate rate (STB/d)

Q = process noise covariance matrix

r_w = wellbore radius (ft)

R = measurement noise covariance matrix

s = skin

t = time

v_k = measurement noise

w_k = process noise

x_k = state vector

y = pressure kernel

z_k = measurement vector

μ = viscosity (cp)

ø = porosity (pore volume/bulk volume)

References

Athichanagorn, S., 1999, “Development of an interpretation methodology for long-term pressure data from permanent downhole gauges”. Stanford University PhD thesis.

Athichanagorn, S., Horne, R.N., and Kikani, J., 2002, “Processing and interpretation of long-term data acquired from permanent pressure gauges”, SPE Reservoir Evaluation & Engineering (October 2002), 384-391.

Gilly, P. and Horne, R.N. 1998, “Analysis of pressure/flowrate data using the pressure history recovery method”, paper SPE 57601 presented at the 1998 SPE Annual technical conference & exhibition, New Orleans, Louisiana, September 27-30.

Murphy, K., 1998, “Kalman filter toolbox for Matlab”.

Nomura, M., 2006, “Processing and interpretation of pressure transient data from permanent downhole gauges”. Stanford University PhD thesis.

Nomura, M. and Horne, R. N., 2009, “Data processing and interpretation of well test data as a non-parametric problem”, SPE paper 120511 presented at the SPE western regional meeting, San Jose, CA, 24-26 March, 2009.

Simon, D., 2009, “Kalman filtering ”

Thomas, O., 2002, “The data as the model: Interpreting permanent downhole gauge data without knowing the reservoir model”. Stanford University MS thesis.

Welch, G. and Bishop G., 2006, “An introduction to the Kalman filter”.

Yu, Z., Ji, L., Zhoumo Z., and Jin, S., 2009, “A combined Kalman filter-discrete wavelet transform method for leakage detection of crude oil pipelines”, paper presented at the ninth international conference on electronic measurement and instruments.